The Journal of the Korean Society of Oceanography
Vol. 30, No. 3, pp. 147-162, June 1995

Tidal Current and Suspended Sediment Transport in the Keum Estuary, West Coast of Korea*

IM SANG OH, TAE-KYONG NA AND CHANG-BOK LEE
Dept. of oceanography, Seoul National University, Seoul 151-742, Korea

錦江 鹽河口에서의 潮流와 浮游堆積物 이동

吳林象, 羅泰景, 李昌馥
서울大學校 海洋學科

The circulation due to tidal current and river discharge, and the associated suspended sediment transport in macrotidal Keum Estuary, were studied through a series of field measurements of tidal currents and suspended sediment concentration at three anchored stations from 1990 through 1992.

From the measurements, the following results were obtained. At the seaward entrance of the estuary, the veritical profiles of the ebb and flood currents were almost symmetric. At the southern channel the flood current was dominant in the whole water column, but in the northern channel the ebb current was dominant in the surface and bottom layers and the flood current was dominant in the intermediate layer. The maximum velocity of the tidal current in the southern channel was 174 cm/s during flood tide in the intermediate layer. The maximum velocity, 148 cm/s in the northern channel also appeared during flood tide in the intermediate layer. However, in the surface and bottom layers, the maximum velocities were 110.6 cm/s during ebb tide and 92.1 cm/s during flood tide, respectively. The type of the Keum Estuary can be categorized to 'Type 3' of Hansen and Rattray's scheme. The water column of the estuary during the flood tide becomes stratified, and after high water the ebb current reduces the density difference and the water column becomes turbulent. The lower layer of the water column is generally turbulent.

The largest sediment flux 20.61 ton/s was found in the southern channel during flood current in the lowest river discharge (May, 1991), while the smallest flux, 0.65 ton/s in the northern channel in the lowest tidal range (July, 1992). The stronger bottom shear velocity for the present study area seems to erode the bottom sediments during the flood tide, and the relatively long duration of the ebb tide to transport the suspended sediments. Under normal river discharge conditions, the suspended sediments are transported mainly through the southern channel. However, under high river discharge condition the suspended sediment transport is dominant through the northern channel.

큰 潮差 지역인 금강 鹽河口의 潮流와 江水流入에 의한 순환과 이에 따른 부유 물질의 이동을 알아보기 위해 1990년부터 1992년까지 세 정점에서 潮流 및 浮游퇴적물질 농도를 관측하였다.

이 염하구의 가장 외해쪽 관측점에서는 漲潮流와 落潮流의 수직 구조는 거의 대칭형을 나타내고 있다. 또, 남측 수로에서는 漲潮流가 全水層을 통해서 우세하나 북측 수로에서는 상층과 저층에서는 落潮流가 우세하고 중층에서는 漲潮流가 우세 하였다. 남측 수로에서의 최대유속은 漲潮流시에 중층에서 174 cm/s이었으며, 북측 수로의 최대 유속도 漲潮流시 중층에서 148 cm/s로 기록되었다. 반면에 표층과 저층에서는 최대유속 110.6 cm/s의 강한 유속이 落潮時에, 92.1 cm/s이 漲潮시에 각각 기록되었다.

Hansen and Rattray의 scheme에 의하면 금강 鹽河口는 Type 3로 분류될 수 있다. 즉 이 鹽河口의 수층은 漲潮流에 의해서 成層化하고 高潮後의 落潮流는 수층간의 밀도차를 줄여서 亂流化한다. 이곳의 저층 흐름은 일반적

*This work was supported by Seoul National University DaeWoo Research Fund during two years of 1990~1991.

으로 난류성이다.
한 조석 週期당 부유물질의 이동량은 潮差와 하천유량에 달려있다고 생각된다. 관측기간중 최대의 부유물질 이동은 하천유량이 최소였던 1991년 5월중 남측 수로 에서의 추정치에서 초당 20.61 톤으로 나타났으며, 최소 이동은 최소 潮差 기간인 1992년 7월에 북측 수로에서 초당 0.65 톤으로 나타났다. 본 연구해역의 강한 해저전단속도는 창조류 기간 동안에 해저퇴적물을 침식시키며, 상대적으로 긴 落潮 기간은 이들 부유퇴적물을 외해쪽으로 운반시키고 있다. 정상적인 강수 유입 조건하에서는 대부분의 부유물질이 남측 수로를 통해서 운반되나 강수의 유입이 많아지는 경우에 는 오히려 북측 수로를 통한 부유물질의 이동이 더 크다.

INTRODUCTION

The Keum Estuary is located on the southwest coast of the Korean Peninsula (Fig. 1). The Keum River is about 400 km long and its drainage area is about 10,000 km^2. A large sand flat exists at the mouth of the estuary, which divides the waterway into two channels: the southern and northern channels. The southern channel is a main navigation channel with a cross-section area of 12,580 m^2 and the northern channel has a relatively smaller sectional area of 4,740 m^2 (Construction Office of Kunsan Harbor, 1991). The average discharge of the Keum River is about 157 m^3/s, and the average annual river discharge is about 6.4×10^9 m^3 (Schubel et al., 1984). Large seasonal variations exist in the discharge. About 60% of its total annual discharge concentrates in the summer rainy season from July to September (Lee, 1985).

The tide of the study area is of a semi-diurnal type with a diurnal inequality. The tidal factor $F=(K_1+O_1)/(M_2+S_2)$ at Kunsan outer harbour is 0.2, which means the area is a semi-diurnal dominant region. During the spring tides, the spring-tidal saline water penetrates up to about 60 km upstream from the mouth before the construction of the salt water dyke (Lee, 1985). The flood currents are generally stronger than the ebb currents. At the seaward entrance of the Keum Estuary, the maximum flood current appears at 2.4~3.1 hours after the low water and the maximum ebb currents shows at 3.5~4.7 hours after the high water (Chung and Bhang, 1984).

Terrigeneous sediments are transported to the sea as suspended load rather than bed load mainly through rivers (Chester, 1990). The suspended sediments are not transported directly to the sea, but to an estuary first which has a particular circulation pattern before they move to the sea. In this process, estuary plays as a reservoir for the sediments in transport. The most significant character of an estuary is due to the mixing of the fresh and sea waters which are different in their physical and chemical natures (Aston and Chester, 1976). Especially in spring tide, the patterns of the transportation and sedimentation of the suspended sediments are much complicated due to the strong tidal current and the wide variations of the river discharges. Lee and Kim (1987) studied the formation of turbidity maximum before the Keum River dyke was constructed. They found that the transport of suspended sediments and the formation of turbidity maximum within the estuary might be related to the tidal ranges and the significant seasonal variations of the discharge of the Keum River.

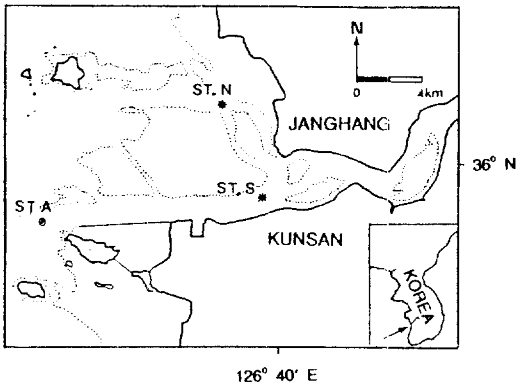

Fig. 1. Map showing the study area, the Keum Estuary. The dotted lines denote the tidal flats, which are exposed at lower low water.

In the present study, the effects of the tidal ranges and river discharges on the transport of suspended sediments will be closely examined in order to clarify the earlier finding(Lee and Kim, 1987) in the estuary. For this purpose, the tidal currents and the

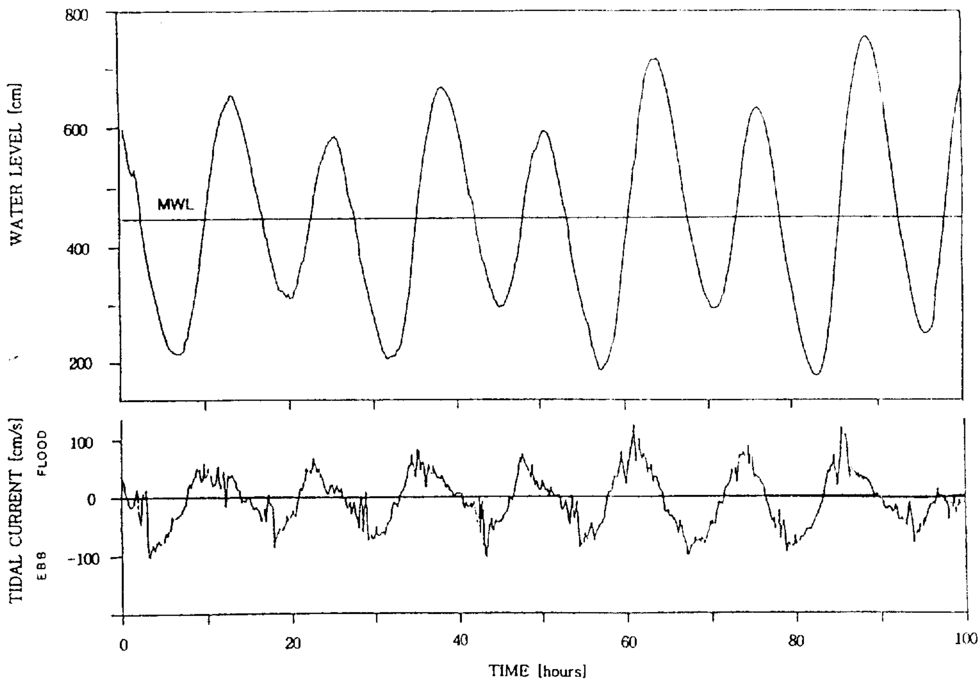

Fig. 2. Tidal elevation (upper curve) and current (lower curve) at St. S. July 20~24, 1990).

concentrations of suspended sediment were directly measured four times (July 1990, May and August 1991, and July 1992) were conducted at three anchor stations (Fig. 1). Two main stations (Sts. S and N) are located in the southern and northern channels, whereas the other station (St. A) is located at the seaward entrance of the estuary. At Sts. S. and N, tidal current velocity and its direction, salinity, and suspended sediment concentration were measured at 3 depths (surface, mid-depth and 1 m above bottom) hourly during one tidal cycle. Especially, during the first survey at the St. S a pressure and current gauge was mounted at the sea bed. At St. A only current vectors were measured. A Braystoke's direct reading current meter (Valeport Co.) was used for the measurements of current velocity and its direction, and T-S bridge and CTD (Sea Bird Electronic Co.) for salinty and temperature, respectively. The suspended sediment concentrations were measured by filtering the water samples through preweighed 0.45 μm GF/C filters.

RESULTS AND DISCUSSIONS

Tides and Tidal Currents

The tide pattern of the study area obtained at St. S is shown in Fig. 2. The two time series, water level and tidal current, show small differences in phase from each other. The tidal current speed generally becomes minimum in high or low water and maximum when the elevation is close to the mean sea level (440 cm for the measurement period). The maximum tidal range during this observation period (July 20~24, 1990) was 5.8 m, and the maximum tidal currents were 120 cm/s during flood and 106 cm/s during ebb.

Fig. 3 shows the vertical profiles of the tidal current velocity at Sts. A, S, and N, observed during the first survey period (July 20~21, 1990). The velocity profiles of the ebb and flood currents at St. A were almost symmetric(Fig. 3A). Considerable residual currents were observed at Sts. N and S. Especially at St. S the flood current was dominant in the whole water column. At St. N ebb current was dominant in the surface and bottom layer while flood current was dominant in the intermediate layer.

The maximum velocity of the tidal current at St. S was 134 cm/s during flood tide in the intermediate

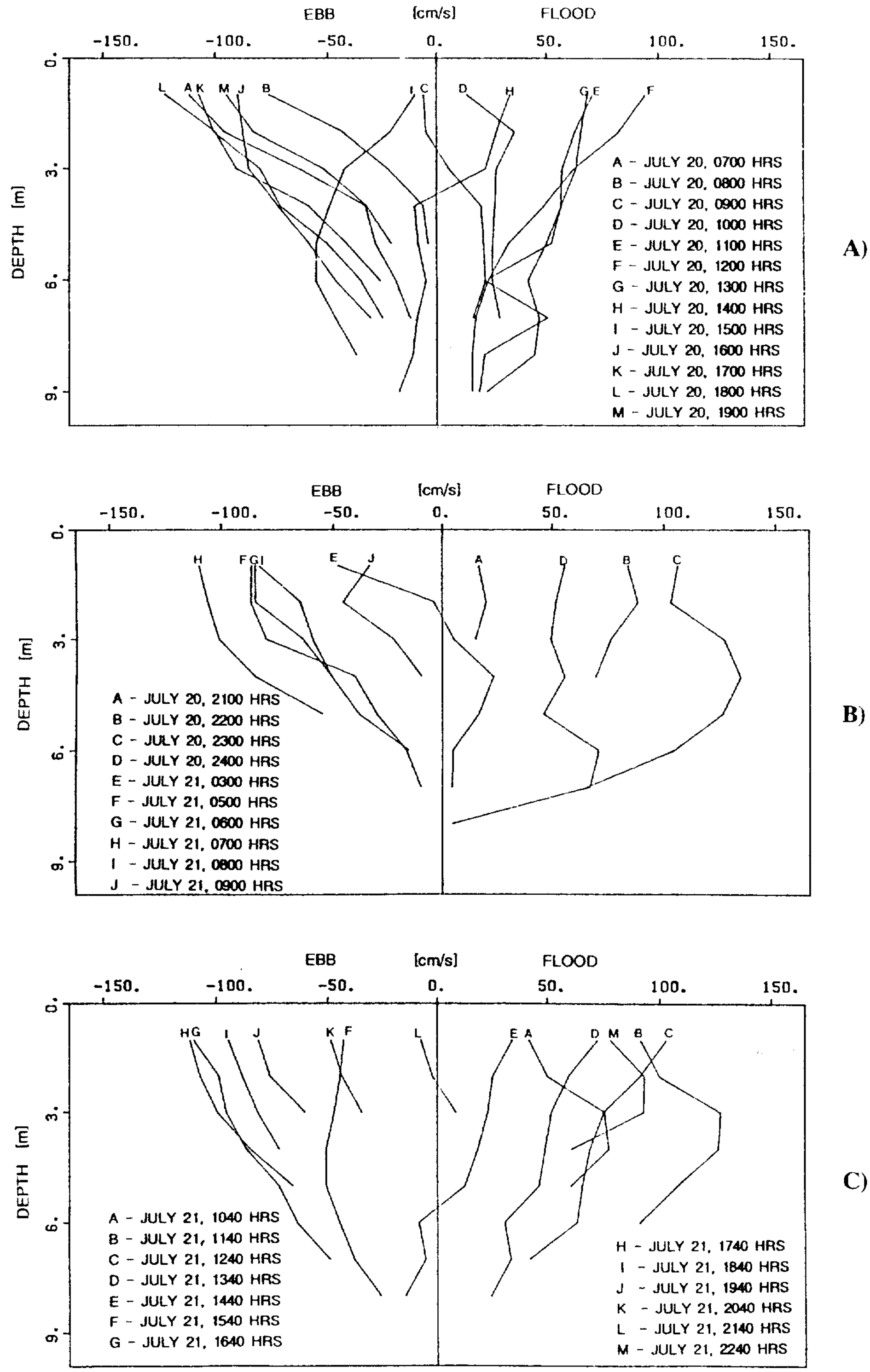

Fig. 3. A) Veritical Profile of tidal current at St. A over a semi-diurnal tidal cycle, B) same as Fig. 3A except at St. S, and C) same as Fig. 3A except at St. N.

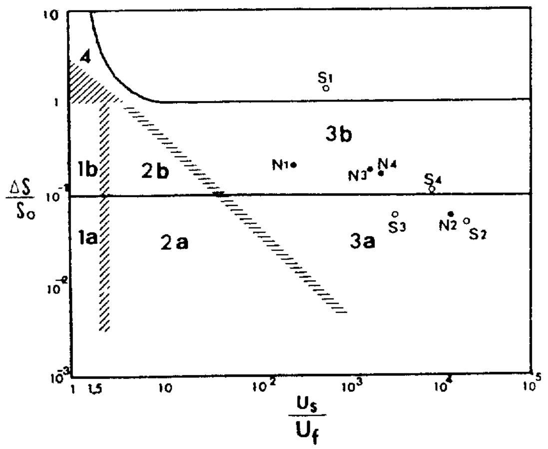

Fig. 4. Stratification-circulation diagram, where S and N represent Sts. S and N, respectively, and the number behing S or N indicates the sequence of the field observation.

layer(Fig. 3B). The maximum velocity, 127 cm/s at St. N also appeared during flood tide in the intermediate layer (Fig. 3C). However, in the surface and bottom layers of the St. N, the maximum velocities were 110.6 cm/s during ebb tide and 92.1 cm/s during flood tide, respectively.

VERTICAL STRATIFICATION

The inflow of fresh water onto the denser seawater in an estuary produces vertical salinity gradients. It is well-known that the salinity gradients result in the estuarine circulation or gravitational convection (Hansen and Rattray, 1966), and that the development of salinity stratification controls the net transport of water and suspended sediment (Allen et al., 1980). Since the Keum Estuary has a wide tidal range, the fluvial and tidal conditions seem to be responsible for the resulting estuarine classification as a sequence of mixing types. There are several approaches to classify estuary according to the degree of mixing between fresh water and sea water (Pritchard, 1955; Simmons, 1955; Hansen and Rattray, 1966). For the present study area, we applied Hansen and Rattray's(1966) scheme which is based on two non-dimensional parameters: stratification and circulation. The stratification parameter $\Delta S/S_o$ is the ratio of the salinity differences of the surface and the bottom layers to the mean salinity of the water column during one tidal cycle. The circulation parameter U_s/U_f denotes the ratio of the mean speed of the tidal current at the surface layer to the river inflow velocity which can be obtained by dividing the river discharge by the cross-sectional area of the estuary. According to this scheme the Keum Estuary can be catagorized to 'Type 3' (Fig. 4). In this type of estuary distinctive two-layer flows become predominant and advective process contributes to more than 99% of the salt transfer.

At this moment, we do not know the overall circulation patterns of the estuary. However, the circulation parameters of the estuary may give us some insights into the mass movement, i.e. a circulation with two layer flows of water movement within the Keum Estuary. From temperature and salinity, we can estimate the vertical stability of a water column. One of the good indicators which can be used as stability index for a water column is Richardson number. The layer Richardson number Ri can be defined as

$$Ri = \frac{gh\, \Delta\rho_m}{U_m^2\, \rho_m} \qquad (1)$$

here ρ_m is layer-mean density of the water column, U_m is layer-mean velocity, and h is the water depth. The Richardson number is the ratio of the potential energy with the kinetic energy, thus, a stable water column has a bigger Ri value. Fig. 5 shows the variations of Ri at St. A over one tidal cycle. During the flood tide, more saline water intrude underneath the less dense upper water, and the water column becomes stratified. After the high tide, the ebb current reduces the density difference and the water column becomes more turbulent and at 16:00 hrs almost the whole column becomes unstable. The circumstance does not last more than an hour. Due to the current speed decrease, the water column becomes stratified shortly. The stratified water in the surface and intermediate layers does not disappear almost all through the tidal cycle. The bottom water is always turbulent.

Table 1 shows the stratification and circulation parameters for each survey period in the Keum Es-

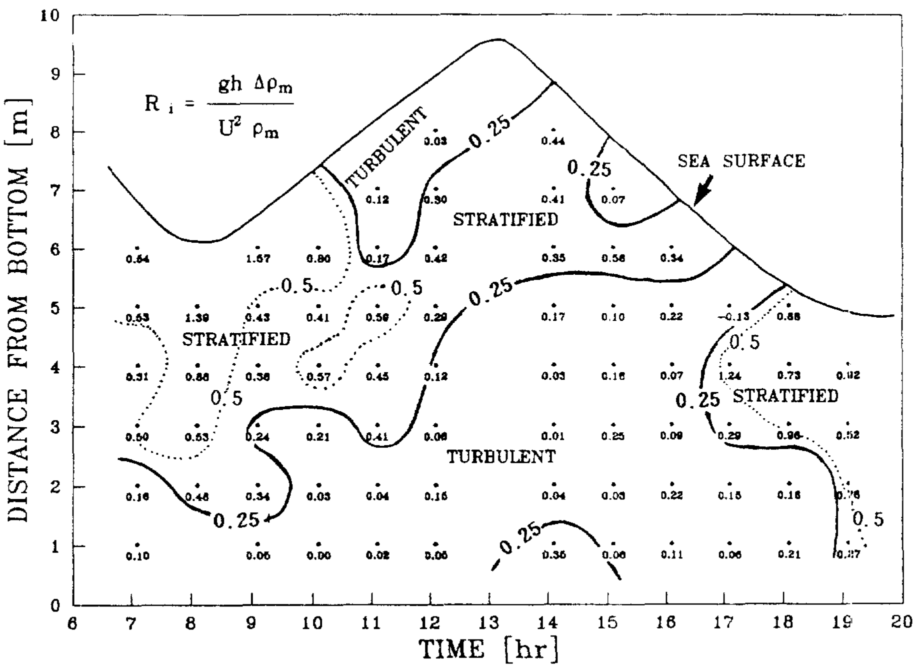

Fig. 5. Layer Richardson number at St. A.

Table 1. Mean values of stratification-circulation parameter

Survey	July 20~21 1990		May 14~15 1991		Aug. 10~11 1991		July 18 1992	
Station	S	N	S	N	S	N	S	N
Stratification	1.25	0.42	0.04	0.02	0.14	0.21	0.11	0.20
Circulation	775	362	29318	10414	4941	1961	9489	2690

tuary. The main controlling factor on the vertical stratification of a water column was found to be a temporal variation of river flow, i.e., the stratification becomes more distinctive with high river discharge (See Table 2 for river discharge). The high river discharge during the first survey in July, 1990, constructs a highly stratified type of salinity, although there are some differences in the stratification from channel to channel. Particularly, relatively large suspended sediment flux during the period at St. N would reflect on the much weaker stratification, which suggests there exists an active turbulent mixing. On the other hand, the well-mixed type of salinity stratification appeared just only under a low river discharge and high tidal range in May, 1991. Extensive turbulent mixing and sediment resuspension would be responsible for that occurrence. In addition, the increased suspended sediment flux in this period with such hydraulic combination agrees well with an optimum condition for the formation of turbidity maximum in the Keum Estuary (Lee and Kim, 1987). From all of our field measurements the well-mixed type of salinity stratification was observed only during the period of low discharge and high tidal range (May, 1991). This means that an extensive turbulent mixing and a sediment resuspension in the study area exists.

Sediment Transport

The time variations of tidal currents, suspended sediment concentration, and salinity of the upper

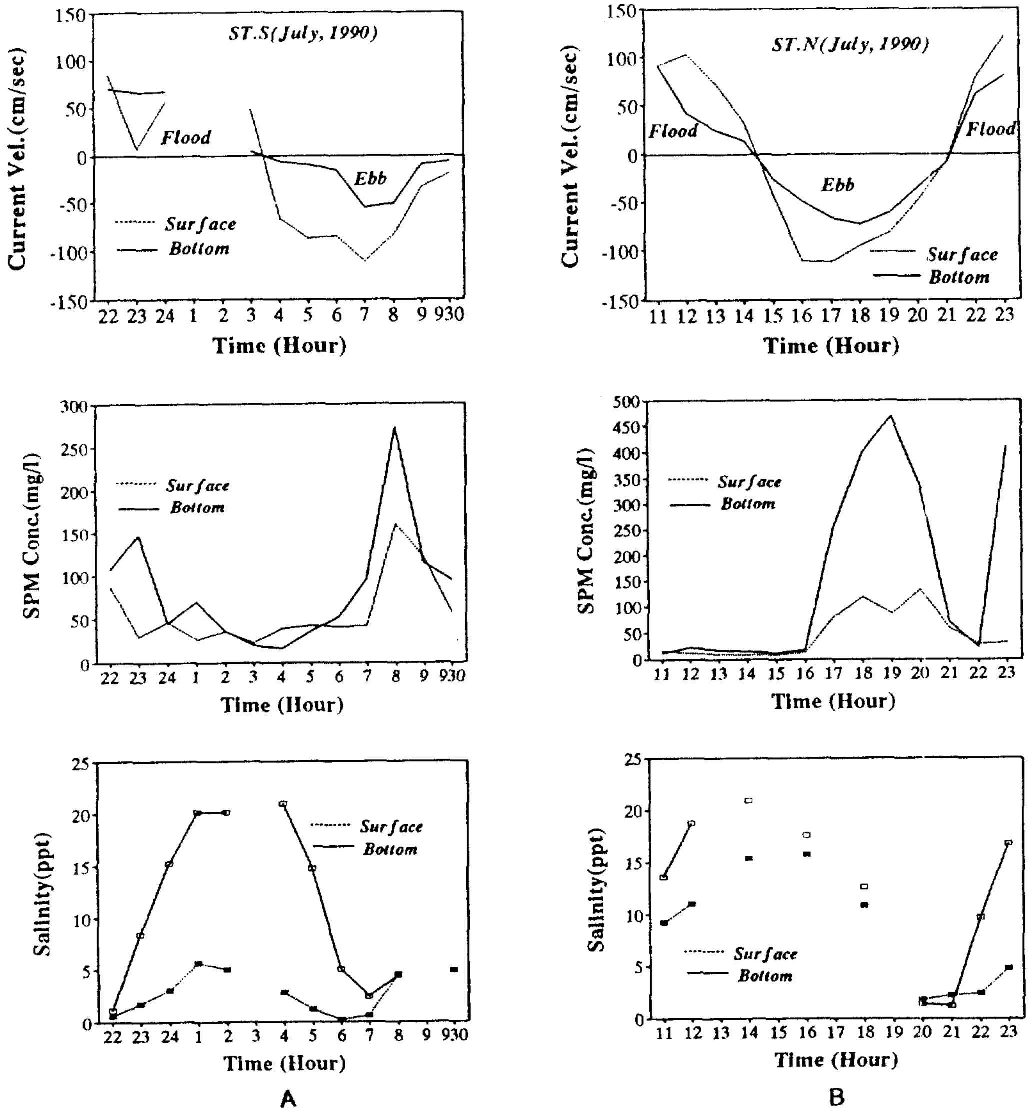

Fig. 6. Time variations of current velocity, suspended sediment concentration and salinity during the first survey (July, 1990) A) at St. S and B) at St. N.

and bottom layers were obtained through this experiment. In the study area, the ebb currents lasted 0.5~2.5 h longer than the flood currents. This longer ebb current did not repeat in every measurement. The velocities of tidal current in the whole water column are stronger in flood tide than those in ebb tide in most of the cases. The highest suspended sediment concentration occurred generally near the time of peak current velocity. The salinity ranges measured over one tidal cycle under different tidal and fluvial conditions show us the relative contribution of fresh water and seawater to the estuarine mixing rate. The contribution of fresh water discharge was greatest during the rainy season (July, 1990), showing the salinity ranging from 5‰ to 20‰ (Fig. 6). Whereas seawater has a dominant influence during the period of low river discharge and higher tidal range of 6.9 m (May, 1991). The salinity ranges

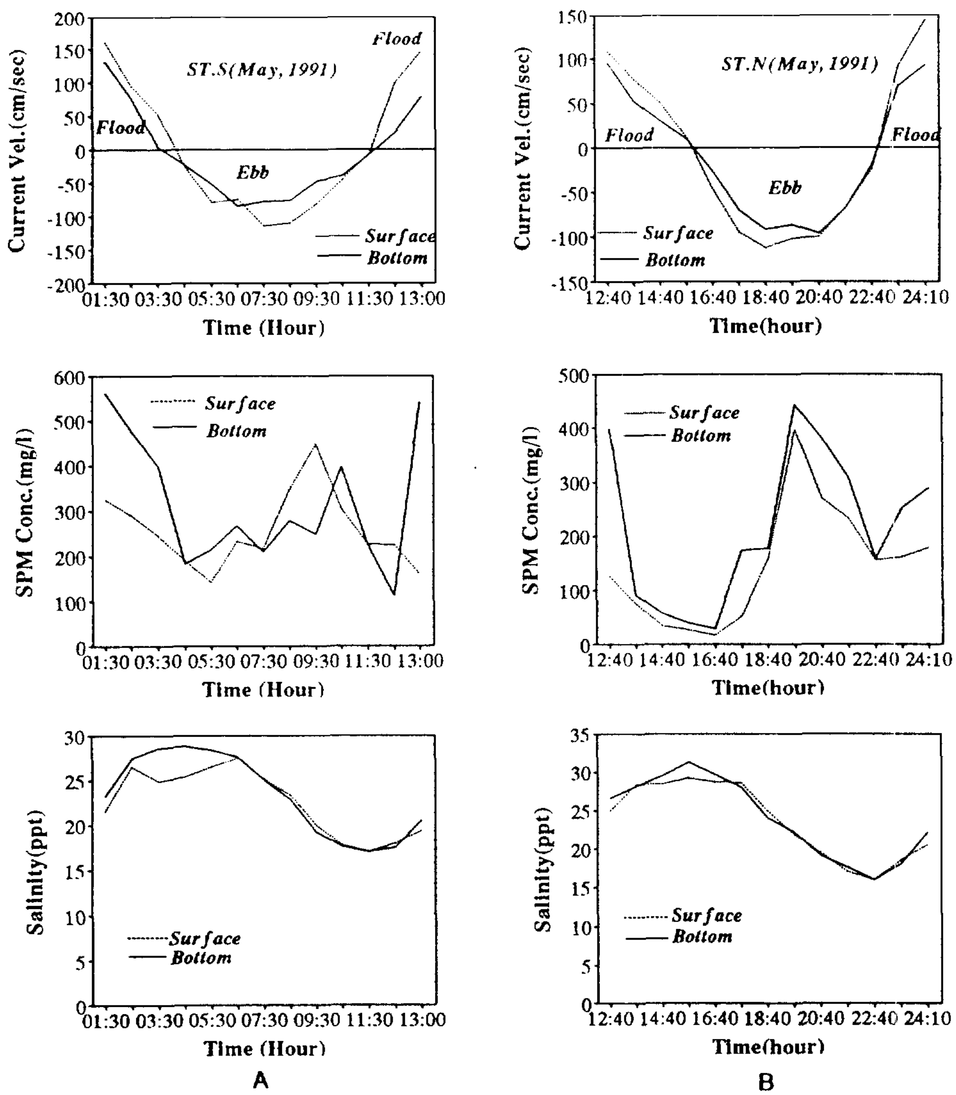

Fig. 7. Time variations of current velocity, suspended sediment concentration and salinity during the second survey (May, 1991) A) at St. S and B) at St. N.

for this period were from about 16‰ to 31‰ (Fig. 7).

The maximum speed of tidal current of the southern channel for each survey is higher than that of the northern channel (Table 2). The maximum SPM concentrations for the two channels also show the similar patterns as the tidal currents. The mean SPM concentration of the bottom layer is the highest, and that of the upper layer is the lowest (Table 2).

The first survey period(July 20~21, 1990) corresponds to a rainy season with river discharge of 1003 m^3/s, and the 5.4 m tidal range. At St. S the maximum current speed and maximum SPM concentration were observed during ebb tide (Fig. 6A). The mean SPM concentration during the ebb was also higher than that during the flood. The average concentrations of the water column over a tidal cycle for the three layers are shown in Table 2. The vertical salinity showed a distinct high stratification

Table 2. Some characteristic values which were obtained in the 4 field surveys.

Survey	July 20~21 1990		May 14~15, 1991		Aug. 10~11, 1991		July 18, 1992	
Station	S	N	S	N	S	N	S	N
Tidal Range [m]	5.4		6.1		7.2		5.4	
Maximum Speed [cm/s]	flood 134	flood 127	flood 160	flood 148	flood 174	ebb 110	ebb 111	flood 97
SPM Concentration Maximum [mg/*l*]	273	469	562	443	1061	883	396	232
SPM Concentration Upper Layer Mean [mg/*l*]	58	46	258	145	247	215	119	52
SPM Concentration Mid-Layer Mean [mg/*l*]	52	64	283	152	351	236	165	56
SPM Concentration Bottom Layer Mean [mg/*l*]	82	158	316	215	472	352	238	100
Salinity [‰]	5~20	0~20	17~30	16~31	3~28	3~34	3~29	6~28
River Discharge Rate [m^3/s]	1003		36		192		91	
Remarks	· Spring tide · Large river discharge · Strongly stratified		· Spring tide · Small river discharge · Homogeneous		· Spring tide · Moderate river discharge · Slightly stratified		· Spring tide · Moderate river discharge · Weakly stratified	

ranging from 5‰ to 20‰, suggesting that the influence of fresh water is significant. The maximum current speed at St. S was slightly faster than that at St. N, but the mean speeds (flood-mean and ebb-mean) were faster in St. N (Fig. 6B). The faster mean flows of St. N seem to give a direct influence on the higher overall SPM level at this station. The vertical gradient of salinity at St. N showed a weaker stratification compared with that of St. S. However, the vertical variation of salinity was within the same range as of St. S.

As compared with the river flow rate in the first survey, the second period (May 14~15, 1991) was under much weaker discharge (36 m^3/s) and higher tidal range (6.1 m). At St. S, the peak current velocity occurred during flood tide and the flood-mean current velocity was stronger at all the water depths than the ebb-mean velocities (Fig. 7A). The maximum concentration of SPM occurred at the time of the peak current velocity. Particularily during the ebb tide, the surface concentration of SPM showed higher values than the bottom concentration for about two hours. This density inversion phenomenon may be due to an effective vertical mixing caused by an increase of turbulence, i.e., the highest ebb current velocity and vertically homogenous salinity distribution for the measurement period. The measured range of salinity of the second observation was much higher value than that of the first. Such a range of salinity over 17‰ suggests that the influence of seawater predominates over fresh water (Table 2). At St. N, the peak current velocities at all three water depths occurred during flood tide while the maximum SPM concentration occurring during the ebb (Fig. 7B). The salinity distribution was vertically homogenous and varied in the range of 16‰ to 31‰ over a tidal cycle.

The third survey (August 10, 1991) was conducted under the conditions of high tidal range and a moderate river discharge (Table 2). The high tidal range and the associated faster current velocity at the both stations result in the highest SPM concentration. For St. S, the flood tidal current has its highest energy with current velocity of 174 cm/s, which corresponds to the fastest current velocity observed during all the survey periods. The observed SPM concentrations were considerably high (Fig. 8A).

At St. N, on the other hand, both the peak current velocity and the highest SPM concentration appeared during the ebb tide. This ebb-dominant tidal asymmetry, as contrasted with the flood-dominant pattern as St. S, seems to be related to the different roles of the northern and southern channels in the estuarine circulation during this period. The highest current velocity was reflected in SPM concentration with a maximum 883 mg/*l* (Fig. 8B). The observed

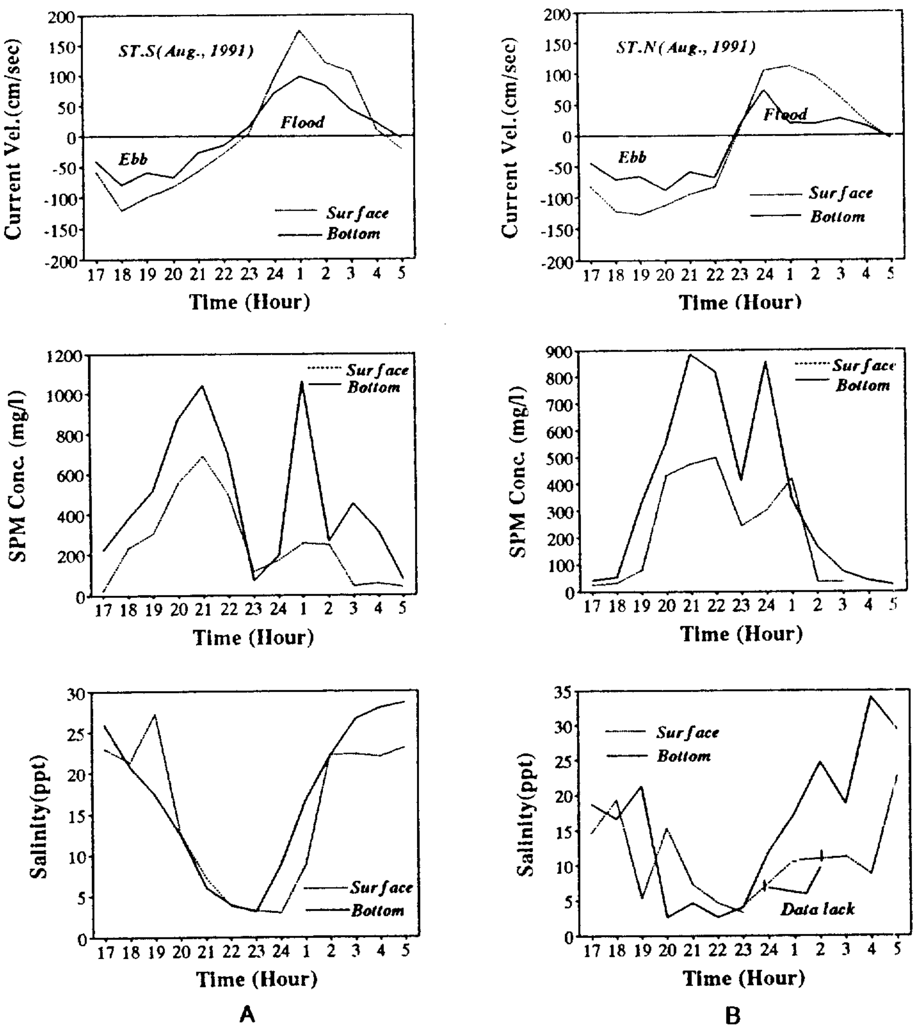

Fig. 8. Time variations of current velocity, suspended sediment concentration and salinity during the third survey (Aug., 1991) A) at St. S and B) at St. N.

salinities at the two stations show a large variation with time, and considerable vertical stratifications.

The fourth survey period (July 18, 1992) was characterized by a moderate river discharge and a high tidal range (Table 2). Both the peak current velocity and the maximum SPM concentration for this period were the lowest among all the field observations. The maximum current velocity and the highest SPM concentration at St. S appeared during ebb tide (Fig. 9A). Ebb-dominant current pattern seems to be due to the longer duration of ebb tide with the peak current velocity. For the St. N, the maximum current velocity and the highest SPM concentration were occurred during flood tide (Fig. 9B). The vertical gradient of salinity was much reduced compared to the former period.

Suspended Sediment Flux

The depth-integrated flux of suspended sediment per a unit cross-sectional length for an hour may be estimated as follows:

$$SSf[g/m]=C_{onc}*V_{el}*W_{id}*T_i \quad (2)$$

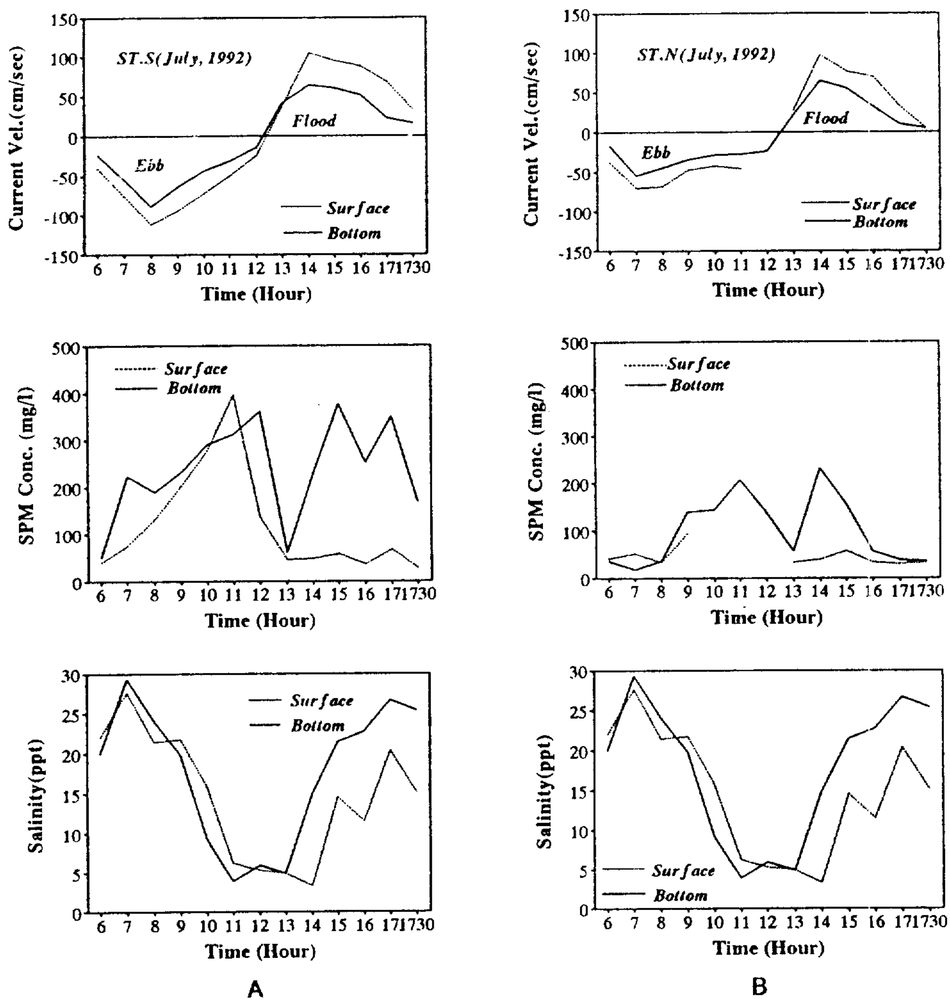

Fig. 9. Time variations of current velocity, suspended sediment concentration and salinity during the fourth survey (July, 1992) A) at St. S and B) at St. N.

where C_{onc} is SPM concentration in g/m^3, V_{el} is current velocity in m/s, W_{id} one third of the total water depth in m, and T_i is time in second.

The depth-integrated transport of suspended sediments at Sts. N and S showed remarkable quantitative differences (Table 3). The sediment flux over a semidiurnal tidal cycle increases with tidal range at both stations. The largest landward and seaward transports in both of the stations appeared during the period of highest tidal range (Aug., 1991), although the landward transport at St. S was largest during the period of the second highest tidal range (May, 1991).

The net transport of suspended sediment was also dependent on the tidal range. The net transport is generally seaward in most of the observation periods. However, the landward flux of suspended sediment was larger than the seaward flux in the second field observation which was under low river discharge and high tidal range of 6.9 m. Generally, stronger flood currents than ebb currents for this observation period were present so that the larger landward flux may result.

More precise recognition of the net transport of suspended sediment through a channel requires the exact estimation of the channel cross-section. No available data to estimate the change of cross-sec-

Table 3. The depth-integrated suspended sediment flux. Positive net flux indicates the landward transport. [ton/m/tide]

Survey	Current	Southern channel	Northern channel
July 20~21 1990	Flood	2.77	2.27
	Ebb	3.04	6.97
	Net	−0.27	−4.70
May 14~15, 1991	Flood	37.09	15.61
	Ebb	24.42	11.35
	Net	12.67	4.26
Aug. 10~11, 1991	Flood	27.82	16.20
	Ebb	28.79	20.20
	Net	−0.97	−4.00
July 18, 1992	Flood	8.58	3.11
	Ebb	13.50	2.42
	Net	−4.92	0.69

Table 4. The suspended sediment flux at each channel. Positive net flux indicates the landward transport. [ton/m/tide]

Survey	Current	Southern channel	Northern channel
July 20~21 1990	Flood	1.82	1.01
	Ebb	2.81	2.88
	Net	0.99	−1.87
May 14~15, 1991	Flood	20.61	4.10
	Ebb	14.69	2.91
	Net	5.92	1.44
Aug. 10~11, 1991	Flood	20.39	4.32
	Ebb	20.18	6.13
	Net	−0.21	−1.81
July 18, 1992	Flood	6.10	0.95
	Ebb	10.10	0.65
	Net	−4.00	0.30

tion of the channels exist at this moment. We, therefore, introduced mean values of the cross-sections averaged over a spring tidal month. The transport of suspended sediment (g/s) through the northern and the southern channels were calculated by multiplying flow area (m^2) by depth-mean current velocity (m/s) and depth-mean suspended sediment concentration (g/m^3), and its result is shown in Table 4. The overall trends show a good similiarity to the previous depth-integrated flux although the calculation of channel flux was a first-order approximation. As the tidal range increases, the channel flux of suspended sediment also increases.

In addition, the sediment flux in suspension through the southern channel which has a wider cross-sectional area is significantly larger than that through the northern channel, except for the high river discharge period, July 1990.

The total flux, the whole sediment transport through the southern and northern channels varies with tidal and fluvial conditions. The largest suspended sediment flux appeared during the period of the highest tidal range, August, 1991. Meanwhile, the total fluxes were seaward for the most of the periods except May, 1991. The longer duration of the ebb tide seems to be responsible for the seaward-dominant transport of the suspended sediment.

The first and fourth field observations with nearly the same tidal range were under different fluvial conditions, an extremely high river discharge (1003 m^3/s) and a moderate river discharge (91 m^3/s), respectively. It is found that the suspended sediment flux with a high river discharge was not higher than that with a moderate discharge. The flux through the southern channel was significantly larger than that through the northern channel for the most part except the seaward flux during the rainy season (July, 1990). Net flux of suspended sediment for the most part was a seaward direction except the period of low river discharge and tidal range of 6.9 m. The longer duration of the ebb tide seems to influence significantly on the seaward transport pattern. The exceptionally large net landward flux of suspended sediment in May, 1991, seems to be caused from much strong flood current for the period.

Tidal Current and Sediment Resuspension

In macrotidal estuaries such as the Keum Estuary, tide plays an important role not only in local scour and sediment resuspension, but also in controlling net sediment transport and sometimes estuary-shelf sediment exchanges (Schubel, 1971; Castaing and Allen, 1981). The erosion and resuspension of bottom sediment in estuaries are related to the intensity of tidal current acting on the estuarine bed. The intensity can be quantified by estimating boundary shear or friction velocity. For fully turbulent flows, the quadratic stress law offers the advantages of simplicity in measuring and application to sediment erosion and resuspension (Sternberg, 1972). Since the flow regime of the Keum Estuary is fully turbulent

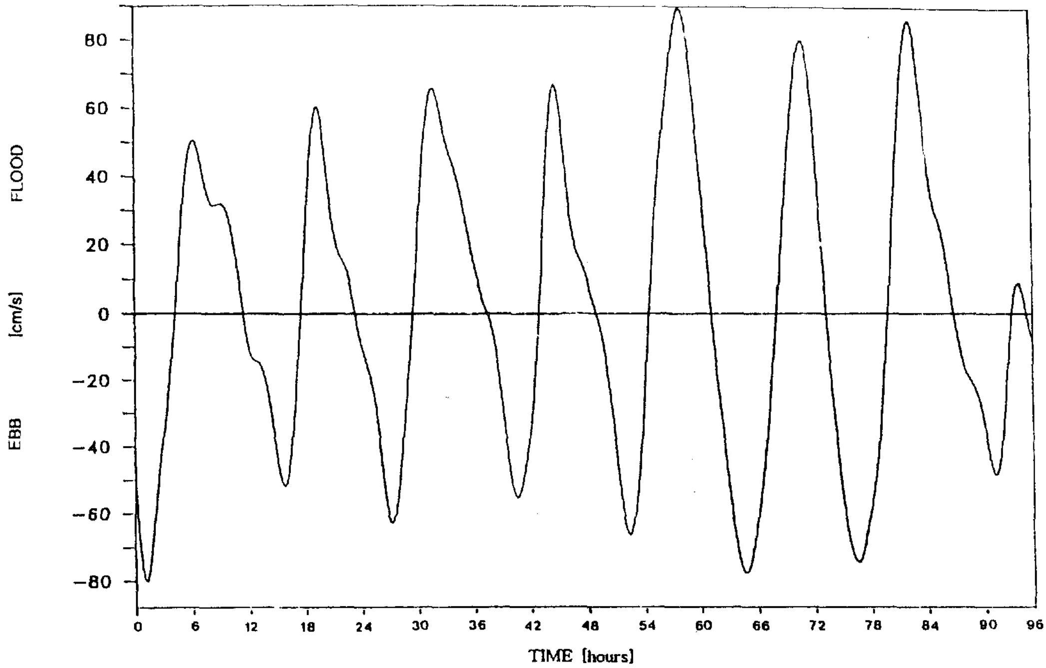

Fig. 10. Smoothed tidal currents at 1.8 m above the sea bed of St. S.

flow (See Fig. 5, also Chung and Bhang, 1984), the conventional terms of quadratic stress law for boundary velocity(U_*) are used for the estimation of sediment transports. Starting from Prandtl's law of turbulent friction and assuming a uniform vertical distribution of internal turbulent stresses, the current profile U is obtained

$$U=(U_*/k)\ln[z/z_o] \qquad (3)$$

where $U_*=(\tau_o/\rho)^{1/2}$ is the shear velocity; τ_o is the bottom shear stress; ρ is the water density; z is vertical coordinate, positive upward and zero at the bottom; z_o is a bottom roughness length factor; and $k\simeq 0.4$ is von Karman constant. The shear stress acting on the bottom is

$$\tau_o=C_d(U_{100})^2 \qquad (4)$$

where C_d is the frictional coefficient; U_{100} is the current speed at 100 cm from sea bottom. Thus the shear velocity can be related directly with the U_{100}

$$U*^2=C_d(U_{100})^2. \qquad (5)$$

Using the relations above, the bottom frictional coefficient is

$$C_d=k^2/[\ln(z/z_o)]^2 \text{ at } z=100 \text{ cm}. \qquad (6)$$

The dominant size of the bottom sediment in the study area is 2~4ϕ (You, 1991), thus, the frictional coefficient, C_d can be estimated to be of 0.001~0.0013, which is in the range of common use. This value is one order smaller than the earlier estimate, 1.6×10^{-2} (Chung and Bhang, 1984) for the Keum Estuary.

The mode of transport, however, may be predicted as a function of grain diameter and bottom current speed. According to Smith and Hopkins(1972), a bottom shear velocity over 1.3 cm/s will erode silts and transport them as bed load. If U_* is between 1.3 and 1.4 cm/s, the sand particles will be transported. Since the dominant grain size of bottom sediment in the study area is in the range of 2~4ϕ, it will be reasonable to take 1.3 cm/s as the critical shear velocity for erosion of the bottom sediment.

The threshold velocity at 100 cm from the flat sea bottom may be estimated by using the diameter of bottom sediment (Miller et al., 1977). The threshold

Table 5. Mean boundary shear velocity acting on the estuarine bed. [cm/sec]

Survey	July 20~21 1990		May 14~15, 1991		Aug. 10~11, 1991		July 18, 1992	
Station	S	N	S	N	S	N	S	N
Tidal mean velocity	4.1	6.1	7.1	7.8	6.1	5.5	5.6	4.1
Flood mean velocity	6.5	6.5	8.1	7.4	6.9	3.5	5.4	3.9
Ebb mean velocity	2.8	5.7	6.5	8.2	5.3	7.3	5.8	4.2

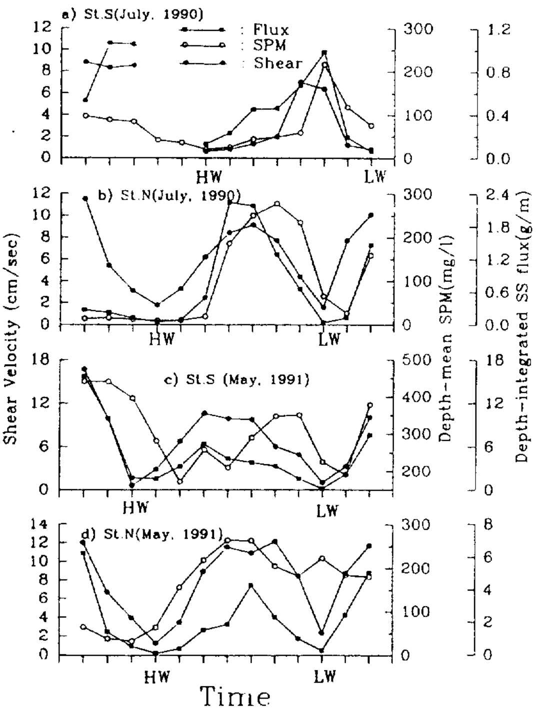

Fig. 11. Time variations of depth-mean suspended sediment concentration and depth-integrated suspended sediment flux over a tidal cycle with boundary shear velocity, a) and b) are from the measurements during July, 1990 at St. S and St. N, respectively, and c) and d) during May, 1991 at St. S. and St. N, respectively. HW and LW in the abscissa stand for high and low water, respectively.

velocity for sediments of 2~3ϕ in diameter is estimated to be 40 cm/s. The duration of the flow velocity over the threshold velocity of 40 cm/s (see Fig. 10) becomes longer as the amplitude of tidal current increases, and becomes more than three hours in the peak amplitude time.

The estimated boundary shear velocities show wide variations depending on the tidal phase and the period of the measurements (Table 5). The mean boundary shear velocities are in the order of 1 to 10 cm/s. About 90% of the estimated U* were higher than the critical shear velocity of 1.3 cm/s, suggesting that most of the sand in the study area are easily eroded and transported for the semidiurnal tidal cycle.

The ebb-mean boundary shear velocity at St. S during the first observation (July, 1990) is much weaker than that at St. N (Table 5). More vigorous bottom turbulence seems to occur during the ebb tide and cause more resuspensions of bottom sediment in the northern channel. The relatively large amount of landward flux during the flood tide at St. N shows that the considerable amount of the high-concentrated sediment suspended during the ebb tide may come back during the following flood tide. For the second field observation, the data of St. N shows a disagreement that the peak current velocity occurs during the flood tide whereas the maximum SPM concentration appears at bottom during the ebb tide (Fig. 7A). Such a trend could be emerged from the different shear velocity acting on the bed during semidiurnal cycle. Much stronger shear velocity lasted for longer time during the ebb tide (Fig. 11(d)). In addition, the occurrence of the strongest shear velocity during the flood has an influence on the considerable increase of landward flux at St. S.

Sediment resuspension is caused not only by the boundary shear velocity but also by the scouring lag effect. The time variations of depth-mean SPM concentraton and depth-integrated suspended sediment flux with changes in boundary shear velocity over one tidal cycle are examined (Fig. 11). In this figure the two surveys (July, 1990 and May, 1991) with considerable differences in river discharge and tidal range are compared. It can be easily noted that there are rapid adjustments of the suspended sediment concentration and their fluxes to the changes in bottom shear velocity. This rapid adjustment is more clearly shown during the slack periods. Such a trend could be seen also from other observations. This aspect seems to result from a rapid sedimentation of SPM. However, during about three hours before high water slack in Fig. 11(b), which corresponds to high river discharge condition, both the SPM concentration and its flux decrease significantly although the shear velocities maintained were much higher than the critical erosion velocity.

There could be some other reasons for the observed low suspended sediment concentration and its flux. One of the reasons may be found in an increased settling velocity due to turbulence-related particle aggregation (Allen et al., 1980), and another reason may be due to flushing of suspended particle away the estuary by high river discharge. The aggregation effect is, however, in contradiction with the notion that the higher turbulence levels associated with the higher currents would produce an increased capacity of suspended sediments and account for higher concentrations (Biggs, 1978). The flushing and dilution effect will be more adequate reasons to explain the phenomenon. The estuarine flushing time of river water was reported to be nearly inversely proportional to fresh water discharge rate (Zimmerman, 1988). The increase in river water discharge in rainy season enhances the seaward transport of suspended sediments and flushs away the suspended loads, resulting in the shortening of residence time of suspended sediments and then dilution in the suspended sediment concentration.

Our field observations lie in different tidally-changing water depth: The water depths employed in our flux calculation are based on in situ measurements in the field observations. Consequently, even though the first period was under rainy season, its shallowest water depth measured among all the field observations reflects smallest amount of suspended sediment transport.

The relatively high filtering efficiency of about 65% of the Keum Estuary (Schubel, et al., 1984) suggests that the suspended sediment introduced into the Keum Estuary is more likely to be deposited within the estuary than to escape seaward. Another evidence of the sedimentation tendency emerges from a continuous expansion of the sand flat which is placed in the middle of the Keum Estuary (Choi et al. 1989).

CONCLUSIONS

The tidal currents and the sediment transport of the Keum Estuary were measured four times (July 1990, May 1991, August 1991, and July 1992) at the three anchor stations. From the measurements, the followings are obtained:

At St. A which is at the seaward entrance of the estuary, the velocity profiles of the ebb and flood currents are almost symmetric. Considerable residual currents are observed at Sts. N and S. Especially in St. S the flood current is dominant in the whole water column. In St. N ebb current is dominant in the surface and bottom layer, while flood current is dominant in the intermediate layer. The maximum velocity at St. S was 138.8 cm/s during flood tide in the intermediate layer. At St. N, the maximum velocity was 134.4 cm/s during flood tide also in the intermediate layer. However, in the surface and bottom layers the maximum velocity were 110.6 cm/s during ebb tide and 92.1 cm/s during flood tide, respectively.

The Keum Estuary can be catagorized as 'Type 3' of Hansen and Rattray's scheme. The water column of the estuary becomes stratified during flood tide, and after high water the water column becomes more turbulent and the density difference of the water column is reduced. The lower layer of the water column is generally more turbulent. The suspended sediment flux in the Keum Estuary depends most significantly on the phase of tide and the river discharge rate. The largest sediment flux, 20.61 ton/s, was found in the southern channel during flood current in the lowest river discharge (May, 1991) while the smallest flux, 0.65 ton/s, in the northern channel in the lowest tidal range (July, 1992).

The net flux of suspended sediment shows dominantly a seaward direction. The relatively stronger bottom shear current during the flood tide seems to erode the bottom sediments, and the bottom current of the longer duration during the following ebb tide seems to transport the suspended sediment seaward.

REFERENCES

Allen, G.P., J.C. Salomon, P. Bsssoullet, Y. Du Penhoat, and C. De Grandpre, 1980. Effects of tides on mixing and suspended sediment transport in macrotidal estuaries. *Sedimentary Geology,* **26**: 69-90.

Biggs, R.B., 1978. Coastal Bays. In: R.A. Davis, Jr., Coastal Sedimentary Environments. Springer-Verlag, New York Inc., p.69-99.

Castaing P. and G.P. Allen, 1981. Mechanisms controlling seaward escape of suspended sediment from the Gironde: A macrotidal estuary in France. *Marine Geology,* **40**: 101-118.

Choi, B.H., K.G. Kang, and S.W. Lee, 1989. Tide and sediment transport in the Keum river estuary. *J. Korean Soc. Coastal and Ocean Engrs,* **1**: 31-43.

Chung, J.Y. and I.K. Bhang, 1984. Circulation dynamics of the Keum river estuary-Fluid dynamic characteristics. *J. Oceanol. Soc. Korea,* **19**: 141-152.

Construction Office of Kunsan Harbor, 1991. Report on Investigation of Hydrological Phenomena in the Keum Estuary, Kunsan, Korea. (in Korean).

Hansen, D.V. and M. Rattray, 1966. New dimensions in estuary classification. *Limnol. Oceanogr.,* **11**: 319-326.

Lee C.B., 1985. Sedimentary processes of fine sediments and the behaviour of associated metals in the Keum estuary, Korea. In: Sigleo, A.C. and A. Hattori. eds. Marine and Estuarine Geochemistry. Lewis, Michigan, pp.209-225.

Lee C.B. and T.I. Kim, 1987. Formation and evolution of turbidity maximum in the Keum estuary, West coast of Korea. *J. Oceanol. Soc. Korea,* **22**: 105-118.

Miller, M.C., I.N. McCave, and P.D. Komar, 1977 Threshold of sediment motion under uni-directional currents. *Sedimentology,* **24**: 507-528.

Pritchard, D.W., 1955. Estuarine circulation patterns. Proc. Amer. Civil Eng., 81, No. 717.

Schubel, J.R., 1971. Tidal variations of the size distribution of suspended sediment at a station in the Chesapeake bay turbidity maximum. *Neth. J. Sea Res.,* 5: 252-266.

Schubel, J.R., H. Shen and M. Park, 1984. A comparison of some characteristics sedimentation processes of estuaries entering the Yellow sea. In: Marine Geology and Physical Processes of the Yellow Sea eds. by Park, Y.A., O.H. Pilkey and S.W.Kim, Seoul, 286-308.

Simmons, H.B., 1955. Some effects of upland discharge on estuarine hydraulics. Proc. Am Soc. Civ. Eng., **81**: 1-20.

Smith, J. D. and T.S. Hopkins, 1972. Sediment transport on the continental shelf off Washington and Oregon in light of recent current measurements, eds. D.J.P. Swift, D.B. Duane, and O. H. Pilkey, Hutchinson and Ross Inc., Dowden, p.143-180.

Sternberg, R.W., 1972. Predicting initial motion and bedload transport of sediment particles in the shallow marine environment. In: D.J.P. Swift, D.B. Duane, and O.H. Pilkey, eds. Shelf Sediment Transport: Process and Pattern, Hutchinson and Ross Inc., p.61-82.

You, D.H. and K.D. Suh, 1982. Evaluation of suspended sediment transport in a macrotidal coastal region. Bulletin of KORDI, **4**: 73-84.

You, S.H., 1991. A study of the trasnport of the suspended sediment in the Keum river estuary, Korea. MS Thesis, Seoul National Univ.(in Korean).

Zimmerman J.T.F., 1988. Estuarine residence times. In: Bjorn Kjerfve. eds., Hydrodynamics of Estuaries, v.1 Estuarine Physics, CRC Press Inc., pp.75-84.

Zimmerman, J. T. F., 1988. Estuarine residence times. In: Bjorn Kjerfve. eds., Hydrodynamics of Estuaries, V. 1 Estuarine Physics, CRC Press Inc., p. 75-84.

Accepted May 30, 1995